

# On the convergence of spherical harmonic expansion of topographic and atmospheric biases in gradiometry

Mehdi ESHAGH<sup>1</sup>

<sup>1</sup> Division of Geodesy, Royal Institute of Technology, Stockholm, Sweden  
e-mail: eshagh@kth.se

**Abstract:** The gravity gradiometric data are affected by the topographic and atmospheric masses. In order to fulfill Laplace-Poisson's equation and to simplify the downward continuation process, these effects should be removed from the data. However, if the analytical downward continuation is considered, the gravity gradients can be continued downward disregarding such effects but the result will be biased. The topographic and atmospheric biases can be expressed in terms of spherical harmonics and studying these biases gives some ideas about analytical downward continuation of these quantities to sea level. In formulation of harmonic coefficients of the topographic and atmospheric biases, a truncated binomial expansion of topographic height is used. In this paper, we show that the harmonics are convergent to the third term of this binomial expansion. The harmonics of the biases on  $V_{zz}$  are convergent to the first term and they are convergent in  $V_{xy}$  for all the terms. The harmonics of the other components of the gravity gradient tensor are convergent to the second terms, while the third terms are only asymptotically convergent. This means that in terrestrial and airborne gradiometry the biases should be computed just to the second order term, while in satellite gravity gradiometry, e.g. GOCE, the third term can also be considered.

**Key words:** asymptotic convergence, atmospheric density model, binomial expansion, external and internal potentials, global spherical harmonic analysis

## 1. Introduction

The gravity gradiometric data can be measured at the Earth's surface, airborne or satellite levels. In order to determine the physical shape of the Earth or the geoid, the gravitational gradients are useful tools. Similar to the other methods the effect of the topographic and atmospheric masses should be removed to make the computational space harmonic and

to smooth the gravitational field. In such a non-topographic and non-atmospheric space, it will be easier to continue the gradients downward to sea level. By removing the topographic and atmospheric effects the equipotential surfaces change. Therefore, these effects should be restored on the results of downward continuation. However, based on analytical continuation (*Moritz, 1980*), these effects may not be removed prior to the computations. The Kungliga Tekniska Högskolan (KTH) geoid determination method was developed based on the analytical continuation. It is well-known as the least-squares modification of the Stokes formula (*Sjöberg 1984, 1991 and 2003*) with additive corrections including the total topographic and atmospheric effects on the geoid. In fact, an approximate geoid is computed using the modified Stokes formula and surface gravity anomalies, and the effects of disregarded topographic and atmospheric masses are subsequently removed from the approximate geoid. Since the data is directly continued downward to sea level without considering the topographic and atmospheric effects, the result of the downward continuation will be biased. These biases are called topographic and atmospheric biases (*Sjöberg 2007; Eshagh and Sjöberg 2008; Eshagh 2009a*). The topographic and atmospheric biases can be considered for the satellite gravity gradiometry data when the gravity gradients are directly continued downward to sea level for local gravity field determination. The use of the gravity field and steady-state ocean circulation explorer (GOCE) data (*ESA, 1999; Albertella et al., 2002; Balmino et al., 1998 and 2001*) for this goal, namely direct analytical downward continuation of the GOCE data and removing the topographic and atmospheric biases from the downward continued data, is promising.

Expressions for the topographic and atmospheric potentials in spherical harmonics are not new. These effects were mostly considered in geoid determination aspects. The topographic effect has been considered by several geodesists (e.g. *Rummel et al., 1988; Martinec et al., 1993; Martinec and Vaníček, 1994; Sjöberg, 1998; Sjöberg and Nahavandchi 1999; Tsoulis, 2001; Heck, 2003; Seitz and Heck, 2003; Sjöberg, 2000, 2007*). The main goal of these efforts was to compute the topographic effect on geoid and terrestrial gravimetric data considering terrain correction. *Wild and Heck (2004a; 2004b)* considered the topographic effect on satellite gradiometry observations. They also considered the second order radial derivative in their computations. *Makhloof and Ilk (2005; 2006)* studied the topographic-

isostatic effects on airborne gravimetry, satellite gravimetry and gradiometry data. More details about their work can be found in *Makhloof (2007)*. *Novák and Grafarend (2006)* presented a method for computing the topographic and atmospheric effects in satellite gravimetry and gradiometry. Atmospheric effect was investigated by *Ecker and Mittermayer (1969)*; *Wallace and Hobbs (1977)*; *Sjöberg (1993, 1998, 1999, 2001 and 2006)*; *Sjöberg and Nahavandchi (2000)*; *Novak (2000)* and *Tenzer et al. (2006)*. *Eshagh and Sjöberg (2008, 2009a, 2009b)* and *Eshagh (2009a; 2009b)* have investigated the atmospheric effect on the satellite gradiometric data. *Sjöberg (2007)* presented the topographic bias in analytical continuation and concluded that for considering the topographic effect on geoid, it is enough to consider the topographic Bouguer shell effect. Later, *Vermeer (2008)* commented on his paper and used the spherical harmonics to prove that *Sjöberg's (2007)* topographic bias is an approximation of the total topographic effect. *Sjöberg (2008)*, in response of *Vermeer (2008)*, mentioned that the spherical harmonic expansion using a binomial expansion of topography to fourth term was not convergent and the spherical harmonic expansion for the topographic bias would not be a correct way to disprove his results. Later on *Sjöberg (2009a; 2009b)* theoretically proved that the topographic bias was exact and even proved that there was no need to consider the terrain correction in geoid computation.

In this paper we review the topographic bias and present the atmospheric biases in spherical harmonics, which is a new subject. The biases are then considered in gravity gradiometry and the mathematical models of the biases are presented for each gravitational gradient which were not investigated before. The convergence of topographic and atmospheric biases on the gradients is numerically studied.

## 2. Background

After adopting the spherical approximation, the topographic and atmospheric external and internal potentials are expressed by the spherical harmonic series as follow:

$$V_{\text{ext}}^{\text{t,a}}(P) = \frac{GM}{R} \sum_{n=0}^{\infty} \left(\frac{R}{r}\right)^{n+1} \sum_{m=-n}^n \left(v_{\text{ext}}^{\text{t,a}}\right)_{nm} Y_{nm}(\Omega), \quad (1a)$$

$$V_{\text{int}}^{\text{t,a}}(P) = \frac{GM}{R} \sum_{n=0}^{\infty} \left(\frac{r}{R}\right)^n \sum_{m=-n}^n \left(v_{\text{int}}^{\text{t,a}}\right)_{nm} Y_{nm}(\Omega), \tag{1b}$$

where  $GM$  is the geocentric gravitational constant,  $R$  is the mean Earth’s radius,  $r$  is the geocentric distance of the point  $P$ ,  $\left(v_{\text{ext}}^{\text{t,a}}\right)_{nm}$  and  $\left(v_{\text{int}}^{\text{t,a}}\right)_{nm}$  are the fully-normalized spherical harmonic coefficients of the external and internal type for either the topographic or the atmospheric potentials with degree  $n$  and order  $m$ , and  $Y_{nm}(\Omega)$  is the fully-normalized spherical harmonics at the spherical angle  $\Omega$  ( $\Omega = (\theta, \lambda)$ ,  $\theta$  is the co-latitude and  $\lambda$  is the longitude of the point  $P$ ) with the following orthogonality property (*Heiskanen and Moritz, 1967, p. 33*):

$$\iint_{\sigma} Y_{nm}(\Omega) Y_{n'm'}(\Omega) d\sigma = 4\pi \delta_{nn'} \delta_{mm'}, \tag{1c}$$

where  $\sigma$  is the total solid angle,  $d\sigma$  is the surface integration element, and

$$\delta_{nn'} = \begin{cases} 1 & n = n' \\ 0 & n \neq n' \end{cases} \text{ and } \delta_{mm'} = \begin{cases} 1 & m = m' \\ 0 & m' \neq m' \end{cases}. \tag{1d}$$

Based on Eq. (1c), the spherical harmonic coefficients  $\left(v_{\text{ext}}^{\text{t,a}}\right)_{nm}$  and  $\left(v_{\text{int}}^{\text{t,a}}\right)_{nm}$  take the form:

$$\left(v_{\text{ext}}^{\text{t,a}}\right)_{nm} = \frac{R}{4\pi GM} \left(\frac{r}{R}\right)^{n+1} \iint_{\sigma} v_{\text{ext}}^{\text{t,a}}(\Omega') Y_{nm}(\Omega') d\sigma, \tag{1e}$$

$$\left(v_{\text{int}}^{\text{t,a}}\right)_{nm} = \frac{R}{4\pi GM} \left(\frac{R}{r}\right)^n \iint_{\sigma} v_{\text{int}}^{\text{t,a}}(\Omega') Y_{nm}(\Omega') d\sigma, \tag{1f}$$

where  $\Omega'$  spherical angle of the integration points.

There are two important assumptions in formulation of the external and internal harmonics: a) the density of the topographic masses is constant, b) the density of the atmospheric masses changes radially. These two assumptions lead to different way of formulation of the topographic and atmospheric potentials. In what follows, we continue the discussion with external and internal types of the topographic potential.

## 2.1. Internal and external harmonics of the topographic potential

If in the formulation of the topographic potential in terms of spherical harmonics the binomial expansion of the topographic heights is truncated to third-order (before spherical harmonic analysis), the internal and external harmonics will have the following forms (see e.g., *Martinec and Vaníček, 1994; Sjöberg, 2000; Eshagh, 2009a*):

$$\left(v_{\text{ext}}^{\text{t}}\right)_{nm} \approx \frac{3\rho^{\text{t}}}{(2n+1)\rho^{\text{e}}} \left[ \frac{H_{nm}}{R} + (n+2) \frac{H_{nm}^2}{2R^2} + (n+2)(n+1) \frac{H_{nm}^3}{6R^3} \right], \quad (2a)$$

and

$$\left(v_{\text{int}}^{\text{t}}\right)_{nm} \approx \frac{3\rho^{\text{t}}}{(2n+1)\rho^{\text{e}}} \left[ \frac{H_{nm}}{R} - (n-1) \frac{H_{nm}^2}{2R^2} + n(n-1) \frac{H_{nm}^3}{6R^3} \right], \quad (2b)$$

where  $\rho^{\text{t}} \approx 2667 \text{ kg/m}^3$  and  $\rho^{\text{e}} \approx 5500 \text{ kg/m}^3$  are the density of the topographic masses and the mean Earth's density, respectively,  $H_{nm}$ ,  $H_{nm}^2$  and  $H_{nm}^3$  are the spherical harmonic coefficients of  $H$ ,  $H^2$  and  $H^3$ , respectively, and  $H$  stands for the topographic heights above sea level (orthometric height).

Formulation of the harmonics of the atmospheric potentials is not as simple as that of topography since the atmospheric density changes radially. The mathematical model of the harmonics depends on the atmospheric density model which is used. Different analytical models were proposed for the atmospheric density, as summarized in the next subsection.

## 2.2. Internal and external harmonics of the atmospheric potential

As mentioned before, the mathematical model of the harmonics of the atmospheric potential depends on the type of the analytical density model used. Here we briefly present some of these analytical models as well as their corresponding internal and external harmonics.

### 2.2.1. The exponential model

An exponential function for the atmospheric density can be considered as (*Lambeck, 1988*):

$$\rho^a(h) = \rho_0 e^{-\alpha' h}, \tag{3a}$$

where  $\rho^a(h)$  is the radial atmospheric density distribution function,  $\rho_0 = 1.2227 \text{ kg/m}^3$  is the atmospheric density at sea level,  $R$  is the mean radius of the Earth,  $h$  is the height of any point above sea level and inside the atmosphere and  $\alpha' = 1.3886 \times 10^{-4} \text{ km}^{-1}$  is a constant.

The external and internal types of harmonics of the atmospheric potential are (Eshagh, 2009a; 2009b):

$$\begin{aligned} (v_{\text{ext}}^a)_{nm} \approx & \frac{3\rho_0}{(2n+1)\rho^e} \left\{ M\delta_{n0} - \frac{H_{nm}}{R} - \frac{n+2-\alpha'R}{2R^2} H_{nm}^2 - \right. \\ & \left. - \frac{(n+2)(n+1-2\alpha'R) + \alpha'^2 R^2}{6R^3} H_{nm}^3 \right\}. \end{aligned} \tag{3b}$$

and

$$\begin{aligned} (v_{\text{int}}^a)_{nm} \approx & \frac{3\rho_0}{(2n+1)\rho^e} \left\{ \left( \frac{1 - Le^{-\alpha'Z}}{\alpha'R} + \frac{1 - e^{-\alpha'Z}}{\alpha'^2 R^2} \right) \delta_{n0} - \frac{H_{nm}}{R} - \right. \\ & \left. - \frac{-n+1-\alpha'R}{2R^2} H_{nm}^2 - \frac{(n-1)(n+2\alpha'R) + \alpha'^2 R^2}{6R^3} H_{nm}^3 \right\}, \end{aligned} \tag{3d}$$

where

$$M = \left[ (1 - Le^{-\alpha'Z}) \left( \frac{2 + \alpha'(R+Z)}{\alpha'^2 R^2} \right) + \frac{2(1 - e^{-\alpha'Z})}{\alpha'^3 R^3} - \frac{Z}{R^2 \alpha'} \right], \tag{3f}$$

$$L = 1 + \frac{Z}{R}. \tag{3g}$$

In formulating the atmospheric potentials (both external and internal types), it is assumed that the atmospheric masses are bounded to a certain altitude above sea level. The topographic masses are replaced by the atmospheric masses which are subtracted from the atmospheric shell from sea level to the upper bound of the atmospheric masses.

### 2.2.2. The power model

The power model is (Sjöberg, 1993):

$$\rho^a(h) = \rho_0 \left( \frac{R}{R+h} \right)^\nu, \quad \text{where } h \geq 0. \tag{4a}$$

The constant  $\nu$  was derived by a simple fitting to the logarithmic scale of the atmospheric density. The Sjöberg fitting (*Sjöberg, 1993*) was based on the model presented by the Reference Atmosphere Committee in 1961 (*Reference Atmosphere Committee, 1961*), and this model was updated based on the United States Standard Atmosphere (1976), by *Eshagh and Sjöberg (2009b)*. In the former case the exponent  $\nu = 850$  was derived, but in the latter (updated) model  $\nu = 930$  was achieved.

The external and internal harmonics of the atmospheric potential based on the power model have the following mathematical forms (*Eshagh, 2009a; 2009b*):

$$\begin{aligned} (v_{\text{ext}}^a)_{nm} \approx & \frac{3\rho_0}{(2n+1)\rho^e} \left\{ \frac{(L^{3-\nu} - 1) \delta_{n0}}{3 - \nu} - \frac{H_{nm}}{R} - \frac{n+2-\nu}{2R^2} H_{nm}^2 - \right. \\ & \left. - \frac{(n+2-\nu)(n+1-\nu)}{6R^3} H_{nm}^3 \right\}, \end{aligned} \tag{4b}$$

and

$$\begin{aligned} (v_{\text{int}}^a)_{nm} \approx & \frac{3\rho_0}{(2n+1)\rho^e} \left\{ \frac{(1 - L^{2-\nu}) \delta_{n0}}{\nu - 2} - \frac{H_{nm}}{R} + \frac{n+\nu-1}{2R^2} H_{nm}^2 - \right. \\ & \left. - \frac{(n+\nu-1)(n+\nu)}{6R^3} H_{nm}^3 \right\}. \end{aligned} \tag{4c}$$

### 2.2.3. The KTH model

This model was proposed by *Eshagh and Sjöberg (2009b)* for the atmospheric density:

$$\rho^a(h) = \begin{cases} \rho_0 [1 + \alpha h + \beta h^2], & 0 \leq h \leq H_0, \\ \rho^a(H_0) \left( \frac{R+H_0}{R+h} \right)^{v''}, & H_0 \leq h \leq Z, \end{cases} \tag{5a}$$

where  $H_0 = 10 \text{ km}$ ,  $\rho^a(H_0) = 0.4127 \text{ kg/m}^3$ ,  $\alpha = -7.6495 \times 10^{-5} \text{ m}^{-1}$ ,  $\beta = 2.2781 \times 10^{-9} \text{ m}^{-2}$  and  $v'' = 890$ . The first part of this model was presented by *Novák (2000)*.

The harmonic formulation of the atmospheric potential based on this model is rather complicated and its external and internal types of harmonics have the following forms (Eshagh and Sjöberg, 2008, 2009b; Eshagh, 2009a):

$$\begin{aligned}
 (v_{\text{ext}}^{\text{a}})_{nm} \approx & \frac{3}{(2n+1)\rho^e} \left\{ \rho_0 \left[ \frac{H_0 \delta_{n0} - H_{nm}}{R} + (n+2 - \alpha R) \frac{H_0^2 \delta_{n0} - H_{nm}^2}{2R^2} + \right. \right. \\
 & \left. \left. + (n+2)(n+1 - 2\alpha R) + 2\beta R^2 \right] \frac{H_0^3 \delta_{n0} - H_{nm}^3}{6R^3} + \right. \\
 & \left. + \frac{\rho(H_0)(K^\nu L^{n+3-\nu} - K^{n+3})}{n+3-\nu} \delta_{n0} \right\} \tag{5b}
 \end{aligned}$$

and

$$\begin{aligned}
 (v_{\text{int}}^{\text{a}})_{nm} \approx & \frac{3}{(2n+1)\rho^e} \left\{ \rho_0 \left[ \frac{H_0 \delta_{n0} - H_{nm}}{R} - (n-1 - \alpha R) \frac{H_0^2 \delta_{n0} - H_{nm}^2}{2R^2} - \right. \right. \\
 & \left. \left. - (1-n)(n+2\alpha R) - 2\beta R^2 \right] \frac{H_0^3 \delta_{n0} - H_{nm}^3}{6R^3} + \right. \\
 & \left. + \frac{\rho(H_0)(K^\nu L^{-n-\nu+2} - K^{-n+2})}{-n-\nu+2} \delta_{n0} \right\}, \tag{5c}
 \end{aligned}$$

where

$$K = 1 + \frac{H_0}{R}. \tag{5d}$$

### 3. Topographic and atmospheric biases in spherical harmonics

The bias is defined as a difference between the downward continued external potential and the internal one at sea level. Mathematically, this idea can be expressed as:

$$V_{\text{b}}^{\text{t,a}}(P) = \left[ V_{\text{ext}}^{\text{t,a}}(P) \right]^* - V_{\text{int}}^{\text{t,a}}(P), \tag{6a}$$

where  $[ ]^*$  stands for downward continuation.  $[V_{\text{ext}}^{\text{t,a}}(P)]^*$  and  $V_{\text{int}}^{\text{t,a}}(P)$  are obtained by considering  $r = R$  in Eqs. (1a) and (1b). Equation (6a) can also be expressed in terms of spherical harmonic series:

$$V_{\text{b}}^{\text{t,a}}(P) = \frac{GM}{R} \sum_{n=0}^{\infty} \sum_{m=-n}^n (v_{\text{b}}^{\text{t,a}})_{nm} Y_{nm}(\Omega), \tag{6b}$$

where  $(v_{\text{b}}^{\text{t,a}})_{nm}$  is the spherical harmonic coefficients of either the topographic or atmospheric biases.

According to Eqs. (2a) and (2b) and the definition of the potential bias in Eq. (6a), we can show that the harmonics of the topographic bias are:

$$(v_{\text{b}}^{\text{t}})_{nm} \approx \frac{3\rho^{\text{t}}}{\rho^{\text{e}}} \left( \frac{H_{nm}^2}{2R^2} + \frac{H_{nm}^3}{3R^3} \right). \tag{7}$$

As Eq. (7) shows,  $(v_{\text{b}}^{\text{t}})_{nm}$  are decreasing as long as  $H_{nm}^2$  and  $H_{nm}^3$  decrease, and consequently there is no problem in the convergence of  $(v_{\text{b}}^{\text{t}})_{nm}$ . However, this is not the case for the atmospheric bias. In what follows, we will mathematically analyze the atmospheric biases based on density models mentioned above.

According to the power model and its harmonics, Eqs. (4b) and (4c), the following harmonic coefficients are obtained for the atmospheric bias (based on Eq. 6a):

$$(v_{\text{b}}^{\text{a}})_{nm} \approx \frac{3\rho_0}{\rho^{\text{e}}} \left\{ \frac{1}{3-\nu} \left[ \frac{ZL^{2-\nu}}{R} + \frac{1-L^{2-\nu}}{2-\nu} \right] \delta_{n0} - \frac{H_{nm}^2}{2R^2} + (\nu-2) \frac{H_{nm}^3}{3R^3} \right\}. \tag{8a}$$

The harmonics of the atmospheric bias based on the exponential density model is obtained by substituting Eqs. (3b) and (3d) into Eq. (6a):

$$(v_{\text{b}}^{\text{a}})_{nm} \approx \frac{3\rho_0}{\rho^{\text{e}}} \left\{ \left[ (2+Z)(1-Le^{-\alpha'Z}) + (1-e^{-\alpha'Z}) \left( \frac{2}{\alpha'R} - 1 \right) \right] \delta_{n0} - \frac{H_{nm}^2}{2R^2} + (\alpha'R-1) \frac{H_{nm}^3}{3R^3} \right\}. \tag{8b}$$

Finally, the harmonics of the atmospheric bias based on the KTH model are obtained by inserting Eqs. (5b) and (5c) into Eq. (6a):

$$\begin{aligned}
 (v_b^a)_{nm} \approx & \frac{3}{\rho^e} \left\{ \rho_0 \left[ \frac{H_0^2}{2R^2} + (1 - \alpha R) \frac{H_0^3}{3R^3} \right] \delta_{n0} + \rho(H_0)K^\nu \times \right. \\
 & \times \left[ L^{2-\nu} \left( \frac{L}{3-\nu} - \frac{1}{2-\nu} \right) - K^{2-\nu} \left( \frac{K}{3-\nu} + \frac{1}{2-\nu} \right) \right] \delta_{n0} - \\
 & \left. - \frac{\rho_0 H_{nm}^2}{2R^2} + (\alpha R - 1) \frac{\rho_0 H_{nm}^3}{3R^3} \right\}. \tag{8c}
 \end{aligned}$$

Until now we have considered the potential bias of the topographic and atmospheric potentials. In this case we assumed that the potentials are given outside the Earth’s surface and after harmonic downward continuation of the potentials to sea level the effects are restored using the corresponding internal types. Now, we shall study the case where the biases are considered on the gradients.

### 4. Topographic and atmospheric biases in gradiometry

The spherical harmonic expansions of the gravitational gradients were presented by *Reed (1973)*. He used the external type of the potential in his expressions. Based on *Reed (1973)* formulas, *Eshagh (2009a)* developed the internal types of the gravitational gradients at sea level. According to our definition of the bias, we define the gradient biases as a difference of the downward continued topographic or atmospheric effects on the gradients to sea level and their corresponding internal type of the effects. According to this definition, we can write (*Eshagh, 2009a*):

$$\begin{aligned}
 \text{bias}V_{zz}^{t,a}(P) = & \frac{GM}{R^3} \sum_{n=0}^{\infty} \sum_{m=-n}^n \left[ (n+1)(n+2) \left( v_{\text{ext}}^{t,a} \right)_{nm} - \right. \\
 & \left. - n(n-1) \left( v_{\text{int}}^{t,a} \right)_{nm} \right] Y_{nm}(\Omega), \tag{9a}
 \end{aligned}$$

$$\begin{aligned} \text{bias}V_{xx}^{\text{t,a}}(P) &= \frac{GM}{R^3} \sum_{n=0}^{\infty} \sum_{m=-n}^n \left\{ \left[ -(n+1) \left( v_{\text{ext}}^{\text{t,a}} \right)_{nm} - n \left( v_{\text{int}}^{\text{t,a}} \right)_{nm} \right] Y_{nm}(\Omega) + \right. \\ &\quad \left. + \left[ \left( v_{\text{ext}}^{\text{t,a}} \right)_{nm} - \left( v_{\text{int}}^{\text{t,a}} \right)_{nm} \right] \frac{\partial^2 Y_{nm}(\Omega)}{\partial \theta^2} \right\}, \end{aligned} \tag{9b}$$

$$\begin{aligned} \text{bias}V_{yy}^{\text{t,a}}(P) &= \frac{GM}{R^3} \sum_{n=0}^{\infty} \sum_{m=-n}^n \left\{ \left[ -(n+1) \left( v_{\text{ext}}^{\text{t,a}} \right)_{nm} - n \left( v_{\text{int}}^{\text{t,a}} \right)_{nm} \right] Y_{nm}(\Omega) + \right. \\ &\quad \left. + \left[ \left( v_{\text{ext}}^{\text{t,a}} \right)_{nm} - \left( v_{\text{int}}^{\text{t,a}} \right)_{nm} \right] \left( \frac{\cos \theta}{\sin \theta} \frac{\partial^2 Y_{nm}(\Omega)}{\partial \lambda \partial \theta} - m^2 \frac{\partial^2 Y_{nm}(\Omega)}{\sin^2 \theta \partial \lambda^2} \right) \right\}, \end{aligned} \tag{9c}$$

$$\begin{aligned} \text{bias}V_{xy}^{\text{t,a}}(P) &= \frac{GM}{R^3} \sum_{n=0}^{\infty} \sum_{m=-n}^n \left[ \left( v_{\text{ext}}^{\text{t,a}} \right)_{nm} - \left( v_{\text{int}}^{\text{t,a}} \right)_{nm} \right] \times \\ &\quad \times \left[ \frac{1}{\sin \theta} \frac{\partial^2 Y_{nm}(\Omega)}{\partial \lambda \partial \theta} - \frac{\cos \theta}{\sin^2 \theta} \frac{\partial Y_{nm}(\Omega)}{\partial \lambda} \right], \end{aligned} \tag{9d}$$

$$\begin{aligned} \text{bias}V_{xz}^{\text{t,a}}(P) &= \frac{GM}{R^3} \sum_{n=0}^{\infty} \sum_{m=-n}^n \left[ (n+2) \left( v_{\text{ext}}^{\text{t,a}} \right)_{nm} - \right. \\ &\quad \left. - (1-n) \left( v_{\text{int}}^{\text{t,a}} \right)_{nm} \right] \frac{\partial Y_{nm}(\Omega)}{\partial \theta}, \end{aligned} \tag{9e}$$

and

$$\begin{aligned} \text{bias}V_{yz}^{\text{t,a}}(P) &= \frac{GM}{R^3} \sum_{n=0}^{\infty} \sum_{m=-n}^n \left[ (n+2) \left( v_{\text{ext}}^{\text{t,a}} \right)_{nm} - \right. \\ &\quad \left. - (1-n) \left( v_{\text{int}}^{\text{t,a}} \right)_{nm} \right] \frac{\partial^2 Y_{nm}(\Omega)}{\sin \theta \partial \theta \partial \lambda}. \end{aligned} \tag{9f}$$

In Eqs. (9a)–(9f),  $\left( v_{\text{ext}}^{\text{t,a}} \right)_{nm}$  and  $\left( v_{\text{int}}^{\text{t,a}} \right)_{nm}$  are the external and internal harmonics of either the topographic or the atmospheric potential, respectively. We already know the mathematical models of  $\left( v_{\text{ext}}^{\text{t}} \right)_{nm}$  and  $\left( v_{\text{int}}^{\text{t}} \right)_{nm}$ ;

see Eqs. (2a) and (2b). Substituting Eqs. (2a) and (2b) into Eqs. (9a)–(9c) and after further manipulations, we can obtain the spherical harmonic coefficients of the topographic biases on the gradients. The atmospheric biases on the gradients can be derived in a similar way. Let us start with the topographic gradient biases in the following section.

### 4.1. Topographic bias on gravitational gradients

We start the discussion with the topographic bias on  $V_{zz}$ . Substituting Eqs. (2a) and (2b) into Eq. (9a) and after further simplifications, we obtain:

$$\left(v_b^t\right)_{nm}^{zz} \approx \frac{3\rho^t}{\rho^e} \left[ \frac{H_{nm}}{R} + (n^2 + n + 4) \frac{H_{nm}^2}{2R^2} + 4(n^2 + n + 1) \frac{H_{nm}^3}{6R^3} \right]. \quad (10a)$$

As Eq. (10a) shows, the harmonics of the topographic bias on the gradient are convergent to the first term. The second and third terms are not convergent or they are asymptotically convergent, meaning that they are convergent until a certain degree and then they diverge.

Equations (9b) and (9c) consist of two parts, the harmonics which are multiplied by  $Y_{nm}(\Omega)$ , and those multiplied by  $\frac{\partial^2 Y_{nm}(\Omega)}{\partial \theta^2}$ . The harmonics of the former is slightly more complicated and needs to be investigated. Here we concentrate on the first part only. Substituting Eqs. (2a) and (2b) into the harmonics of the first part of Eqs. (9b) and (9c), we obtain the following expression:

$$\left(v_b^t\right)_{nm}^{xx} = \left(v_b^t\right)_{nm}^{yy} \approx -\frac{3\rho^t}{\rho^e} \left[ \frac{H_{nm}}{R} + \frac{H_{nm}^2}{R^2} + \left(n^2 + 3 + \frac{n-1}{2n+1}\right) \frac{H_{nm}^3}{6R^3} \right]. \quad (10b)$$

Equation (10b) shows that the first and second topographic terms are convergent, but it can be asymptotically convergent to the third term.

Substituting Eqs. (2a) and (2b) into Eqs. (9e) or (9f) will lead to the same harmonics, namely:

$$\left(v_b^t\right)_{nm}^{xz} = \left(v_b^t\right)_{nm}^{yz} \approx \frac{3\rho^t}{\rho^e} \left[ \frac{H_{nm}}{R} + \frac{3H_{nm}^2}{2R^2} + (n^2 + n + 4) \frac{H_{nm}^3}{6R^3} \right]. \tag{10c}$$

The first two terms in the squared brackets express the topographic bias and we can conclude that the harmonics are convergent to the second topographic term. Again, we observe the divergence in the third term.

Repeating the same process for Eq. (9d) yields the following expression for the harmonics

$$\left(v_b^t\right)_{nm}^{xy} \approx \frac{3\rho^t}{\rho^e} \left( \frac{H_{nm}}{2R^2} + \frac{H_{nm}^2}{3R^3} \right), \tag{10d}$$

which are convergent.

Equation (10a) shows that if we aim to consider the topographic bias on  $V_{zz}$ , we should not use the second and third topographic terms. Equations (10b) and (10c) suggest using the first two terms for computing the topographic bias on  $V_{xx}$  and  $V_{yy}$ , and  $V_{xz}$  and  $V_{yz}$ . No difficulty in convergence is observed in the harmonics of topographic bias on  $V_{xy}$ .

### 4.2. Atmospheric bias on gravitational gradients

Investigation of the atmospheric bias on the gravitational gradients is similar to that of the topographic bias, but depends on the type of the atmospheric density model. Therefore, we study the biases based on each model. Let us start with the power model. The atmospheric bias on  $V_{zz}$  based on this model is:

$$\left(v_b^a\right)_{nm}^{zz} \approx \frac{3\rho_0}{\rho^e} \left\{ \frac{2\delta_{n0}}{3-\nu} \left[ L^{3-\nu} - 1 \right] - 2\frac{H_{nm}}{R} - (n^2 + n + 4 - 2\nu) \frac{H_{nm}^2}{2R^2} + \left[ -4(n^2 + n + 1) + 2\nu(n^2 + n + 3) - 2\nu^2 \right] \frac{H_{nm}^3}{6R^3} \right\}. \tag{11a}$$

Again, we see that the second and third topographic terms are not convergent. The atmospheric bias on  $V_{xx}$  and  $V_{yy}$  based on the power model is:

$$\left. \begin{matrix} \left(v_b^a\right)_{nm}^{xx} \\ \left(v_b^a\right)_{nm}^{yy} \end{matrix} \right\} \approx \frac{3\rho_0}{\rho^e} \left\{ \frac{\delta_{n0}}{3-\nu} \left[ 1 - L^{3-\nu} \right] + \frac{H_{nm}}{R} + (2-\nu) \frac{H_{nm}^2}{R^2} + \right.$$

$$+ \left( n^2 + n + 2 - 3\nu + \nu^2 \right) \frac{H_{nm}^3}{6R^3} \Bigg\}. \tag{11b}$$

Equation (11b) converges to its second topographic term. The atmospheric bias on  $V_{xz}$  and  $V_{yz}$  based on the power model is:

$$\left. \begin{matrix} (v_b^a)^{xz} \\ (v_b^a)^{yz} \end{matrix} \right\} \approx \frac{3\rho_0}{\rho^e} \left\{ \left[ \frac{2(L^{3-\nu} - 1)}{3 - \nu} - \frac{L^{2-\nu} - 1}{2 - \nu} \right] \delta_{n0} - \frac{H_{nm}}{R} + (\nu - 3) \frac{H_{nm}^2}{2R^2} + \right. \\ \left. - (n^2 + n + 4 - 5\nu + \nu^2) \frac{H_{nm}^3}{6R^3} \right\}. \tag{11c}$$

A similar conclusion as that concluded for Eq. (11b) can be made for Eq. (11c).

If the exponential density model is considered for the atmospheric masses, the atmospheric bias on  $V_{zz}$  can be shown to take the form:

$$(v_b^a)^{zz} \approx \frac{3\rho_0}{\rho^e} \left\{ 2M\delta_{n0} - 2\frac{H_{nm}}{R} - (n^2 + n + 4 - 2\alpha'R) \frac{H_{nm}^2}{2R^2} + \right. \\ \left. + \left[ -4(n^2 + n + 1) + 2\alpha'R(n^2 + n + 4) - 2\alpha'^2R^2 \right] \frac{H_{nm}^3}{6R^3} \right\}, \tag{12a}$$

where  $M$  was already defined in Eq. (3f). The atmospheric bias on  $V_{xx}$  and  $V_{yy}$  based on the exponential model is:

$$\left. \begin{matrix} (v_b^a)^{xx} \\ (v_b^a)^{yy} \end{matrix} \right\} \approx \frac{3\rho_0}{\rho^e} \left\{ -M\delta_{n0} - \frac{H_{nm}}{R} + (\alpha'R - 2) \frac{H_{nm}^2}{R^2} - \right. \\ \left. - (n^2 + n + 2 + 4\alpha'R - \alpha'^2R^2) \frac{H_{nm}^3}{6R^3} \right\}, \tag{12b}$$

and the atmospheric bias on  $V_{xz}$  and  $V_{yz}$  based on this model is:

$$\left. \begin{matrix} (v_b^a)^{xz} \\ (v_b^a)^{yz} \end{matrix} \right\} \approx \frac{3\rho_0}{\rho^e} \left\{ \left[ \frac{(4 + 2Z + \alpha'R)(1 - Le^{-\alpha'Z})}{\alpha'^2R^2} + (1 - e^{-\alpha'Z}) \times \right. \right. \\ \left. \left. \times \left( \frac{4}{\alpha'R} - 1 \right) - 2Z\alpha' \right] \delta_{n0} - \frac{H_{nm}}{R} + (\alpha'R - 3) \frac{H_{nm}^2}{2R^2} - \right.$$

$$- \left( n^2 + n + 4 - 6\alpha'R + \alpha'^2 R^2 \right) \frac{H_{nm}^3}{6R^3} \Big\}. \tag{12c}$$

Similar interpretation as those for Eqs. (11a)–(11c) can be made for Eqs. (12a)–(12c).

In a similar way we can obtain the atmospheric bias based on the KTH model, although it is slightly complicated but the strategy of the derivations of the harmonics is the same as that is for the other density models. The bias on  $V_{zz}$ ,  $V_{xx}$ ,  $V_{yy}$ ,  $V_{xz}$  and  $V_{yz}$  are:

$$\begin{aligned} (v_b^a)_{nm}^{zz} \approx & \frac{3}{\rho^e} \left\{ 2(A + B)\delta_{n0} - \left[ \frac{H_{nm}}{R} + (n^2 + n + 4 - 2\alpha R) \frac{H_{nm}^2}{2R^2} + \right. \right. \\ & \left. \left. + (-4(n^2 + n + 1) + 2\alpha R(n^2 + n + 4) - 4\beta R^2) \frac{H_{nm}^3}{3R^3} \right] \rho_0 \right\}, \tag{13a} \end{aligned}$$

$$\begin{aligned} \left. \begin{aligned} (v_b^a)_{nm}^{xx} \\ (v_b^a)_{nm}^{yy} \end{aligned} \right\} \approx & \frac{-3}{\rho^e} \left\{ (A + B)\delta_{n0} - \left[ \frac{H_{nm}}{R} + (\alpha R - 2) \frac{H_{nm}^2}{2R^2} + \right. \right. \\ & \left. \left. + (n^2 + n + 2 - 4\alpha R - 2\beta R^2) \frac{H_{nm}^3}{3R^3} \right] \rho_0 \right\}, \tag{13b} \end{aligned}$$

and

$$\begin{aligned} \left. \begin{aligned} (v_b^a)_{nm}^{xz} \\ (v_b^a)_{nm}^{yz} \end{aligned} \right\} \approx & \frac{3}{\rho^e} \left\{ (A + B - C)\delta_{n0} - \left[ \frac{H_{nm}}{R} + (\alpha R - 3) \frac{H_{nm}^2}{2R^2} + \right. \right. \\ & \left. \left. + (n^2 + n + 4 - 6\alpha R + 2\beta R^2) \frac{H_{nm}^3}{3R^3} \right] \rho_0 \right\}, \tag{13c} \end{aligned}$$

where

$$A = \rho_0 \left[ \frac{H_0}{R} + (2 - \alpha R) \frac{H_0^2}{2R^2} + 2 \left( 1 - 2\alpha R + 2\beta R^2 \right) \frac{H_0^3}{3R^3} \right], \tag{13d}$$

$$B = \frac{\rho(H_0) K^\nu (L^{3-\nu} - K^{3-\nu})}{3 - \nu} \quad \text{and} \quad C = \frac{\rho(H_0) K^\nu (L^{2-\nu} - K^{2-\nu})}{2 - \nu}. \tag{13e}$$

## 5. Numerical studies

In order to numerically study the convergence of the harmonic expansion of the atmospheric potential, we use the delivered topographic model from the shuttle radar topography mission (*Wieczorek, 2007*) global topographic model and generate  $H_{nm}$ ,  $H_{nm}^2$  and  $H_{nm}^3$  in a global spherical harmonic analysis to the degree and order 2160, corresponding to  $5' \times 5'$  resolution. The harmonics  $H_{nm}$ ,  $H_{nm}^2$  and  $H_{nm}^3$  are used to generate degree variances of each topographic term. In the following, we present the degree variances of external and internal harmonics of the atmospheric potential and then we consider the atmospheric bias.

### 5.1. Numerical studies on atmospheric potentials and bias

The degree variances of the external and internal atmospheric potentials based on the aforementioned density models are computed and plotted for better investigation of the topographic terms.

Figures 1a and 1b show the degree variances of each term of the external and internal atmospheric potentials, respectively, based on the exponential model. Unexpected changes are seen in Fig. 1a for the second and third terms of the external harmonics. As can be seen, the values of these terms are decreasing before a certain degree and increasing beyond. If we consider Eq. (3a) at the constant  $\alpha' = 1.3886 \times 10^{-4}$ , we see that its multiplication by  $R = 62378137$  gives 885.67. As the figure shows, the second and third terms are very small around this degree. According to Eq. (3b) one can see that the coefficient of the second term is  $n + 2 - \alpha'$ , which will be very small when  $n = 883$ . The reason for the third term is similar. This is due to the binomial expansion of the topographic heights for deriving the harmonics of the external atmospheric potentials. Figure 1b shows the internal type of the harmonics and, as can be seen, the second and third terms will have more or less the same power as the first term around the degrees 1700 and 2000, meaning that the internal series of the harmonics do not converge for higher degrees. Similar interpretation can be made for Figs. 2a and 2b for the power model when  $\nu = 850$ . As for the harmonics of the KTH model, we can say that both the external and internal series are convergent for the degrees below 2000, but not for higher.

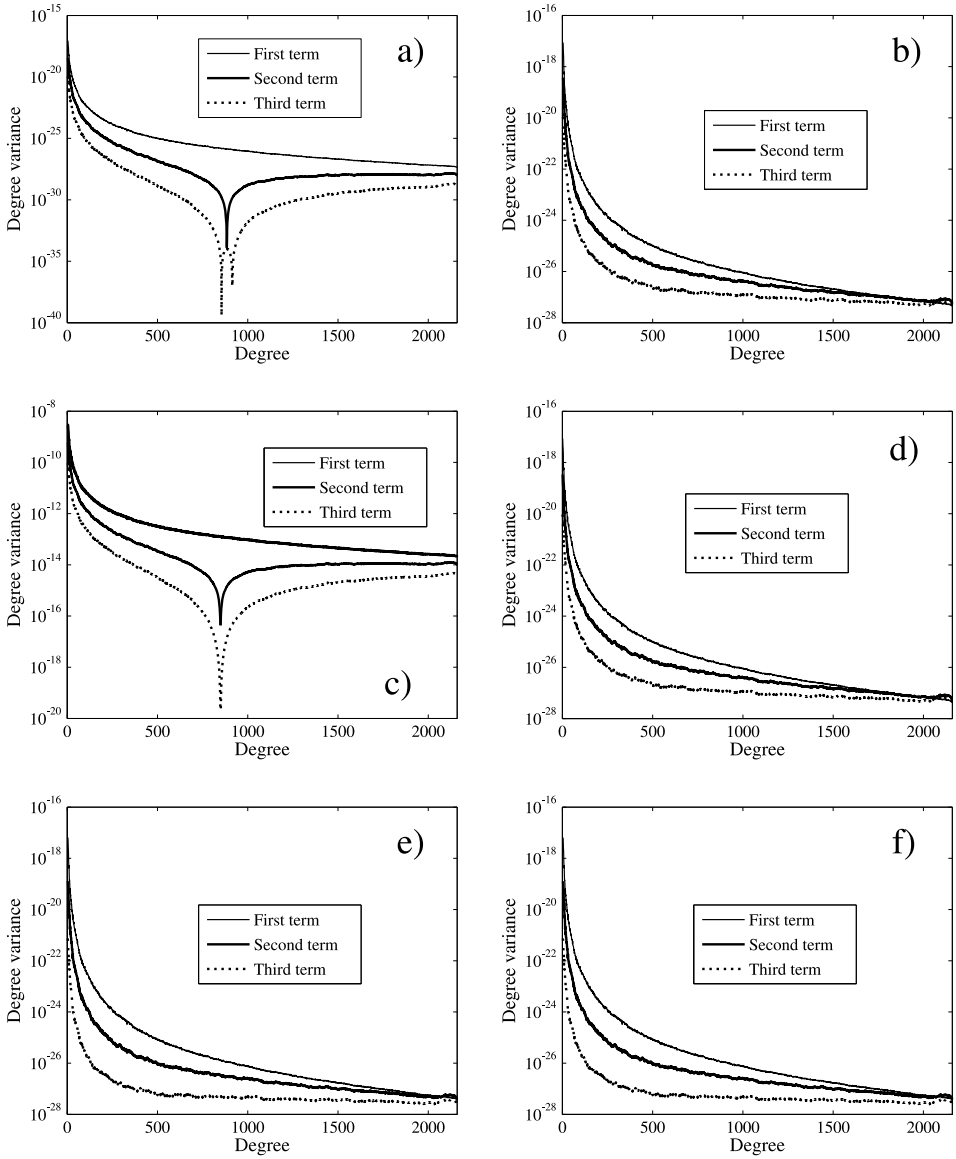


Fig. 1. Degree variances of each topographic term of external and internal harmonics based on a) and b) the exponential model, c) and d) the power model and e) and f) the KTH model.

Now, we consider the atmospheric bias based on the aforementioned density models. Here we use Eqs. (8a)–(8c) and consider the terms related to the topographic harmonics. As can be seen in the equations, the first topographic term of the atmospheric biases is the same for harmonics of all the density models. Also, the second topographic term decays and therefore the atmospheric biases based on these models are convergent. In order to make a better comparison, we plot the degree variances of each topographic term.

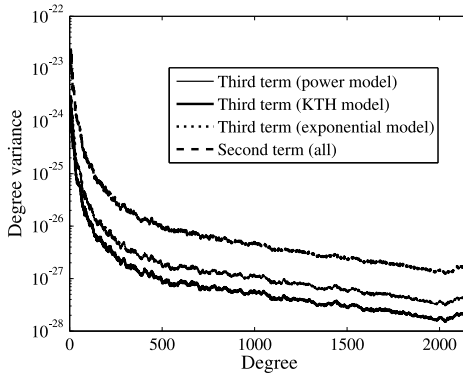


Fig. 2. Degree variances of second and third topographic terms of atmospheric bias based on different atmospheric models.

As already mentioned, the second term of the topographic and the atmospheric biases is the same for all atmospheric models; this is why only one curve is visible for this term in Fig. 2. The harmonics of the exponential and the power density models coincide since the topographic terms of the external and internal are very similar and only one curve is visible for their third bias term. However, the KTH model differs from these two models in the third term.

One consequence of Fig. 2 could be the difference between the atmospheric effect in the remove-compute-restore scheme and the analytical continuation. As can be seen, the internal harmonics of the exponential and power models do not converge above the degree 2000. Therefore we can say that in the remove-compute-restore scheme we are restricted to use the internal type of the harmonics to a certain degree to restore the atmospheric effect. However, as we already mentioned, there is no difficulty in convergence of the atmospheric bias.

### 5.2. Numerical studies on topographic bias on gravitational gradients

Now we plot the degree variances of each topographic term of the topographic bias on the gradients. It was already mentioned that the topographic bias on  $V_{zz}$  is not convergent to the second and third terms. Figure 3a shows that the power of the second term will be the same as that of the first at the degree 58, and the third one is 1520. It means that it is only asymptotically convergent to the degree 58. Equations (10b) and (10c) indicate the divergence of the third term, but Figures 3b and 3c show that this term can also be used as long as the power of the third term is lower than the other terms. Figure 3b shows that it can be used to the degree 66 for  $V_{xx}$  and  $V_{yy}$ , and Figure 3c to 114 for  $V_{xz}$  and  $V_{yz}$ .

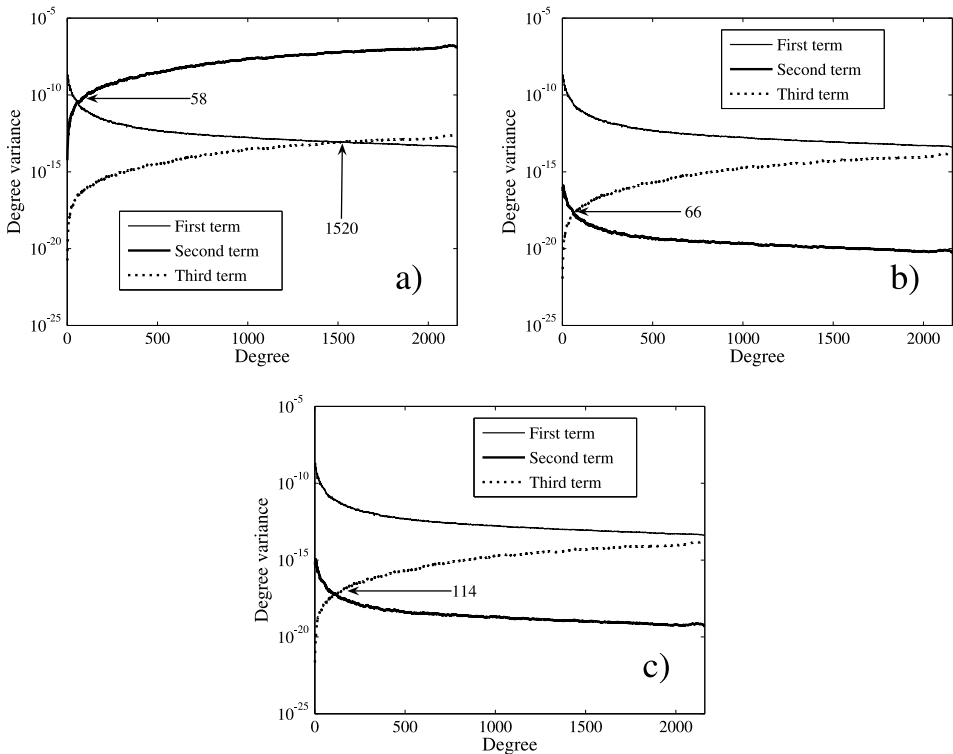


Fig. 3. Degree variances of each topographic term of topographic bias on a)  $V_{zz}$ , b)  $V_{xx}$  and  $V_{yy}$  and c)  $V_{xz}$  and  $V_{yz}$ .

### 5.3. Numerical studies on atmospheric bias on gravitational gradients

In this section, we will consider the atmospheric biases based on the considered density models. We divide this section into three parts and in each part we consider one atmospheric density model. We start with the power model.

#### 5.3.1. The power model

We plot the degree variances of the first, second and third topographic terms of Eqs. (11a)–(11c). Figure 4a shows that the atmospheric bias on  $V_{zz}$  is convergent only to the first topographic term, but the second and third terms are convergent to the degrees 95 and 114, respectively, as the power

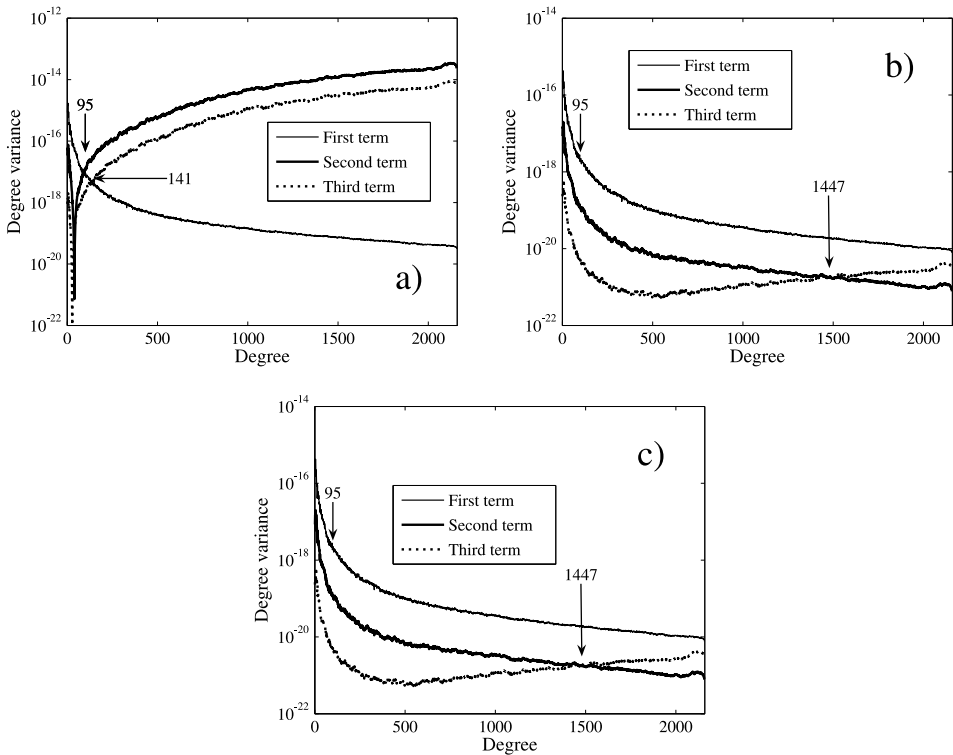


Fig. 4. Degree variances of each topographic term of atmospheric bias based on power model on a)  $V_{zz}$ , b)  $V_{xx}$  and  $V_{yy}$  and c)  $V_{xz}$  and  $V_{yz}$ .

of these terms is the same in the first term on these degrees. Figures 4b and 4c show that the harmonics are convergent to the second topographic term and asymptotically converge to the third term with the degrees below 1447 on  $V_{xx}$ ,  $V_{yy}$ ,  $V_{xz}$  and  $V_{yz}$ .

5.3.2. The exponential model

The same difficulty as that of the power model is observed in convergence of the atmospheric bias for  $V_{zz}$ . As shown in Fig. 5a, the second and third topographic terms have the same power as the first term in the degrees 88 and 95. According to Fig. 5b one observes no problem in convergence of the first and second topographic terms of the harmonics of atmospheric bias on

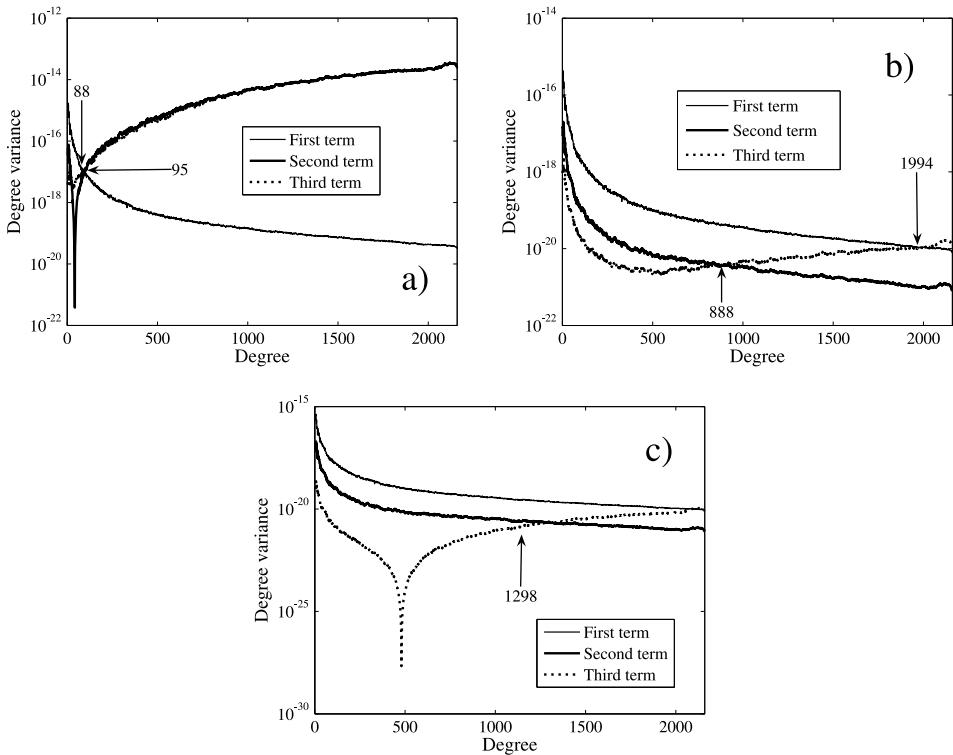


Fig. 5. Degree variances of each term of atmospheric bias based on exponential model on a)  $V_{zz}$ , b)  $V_{xx}$  and  $V_{yy}$  and c)  $V_{xz}$  and  $V_{yz}$ .

$V_{xx}$  and  $V_{yy}$ , but the power of the third term is equal to the first and second terms in the degrees 888 and 1994, respectively. Figure 5c shows that the second topographic term has equal power to that of the second term in the degree 1298.

5.3.3. The KTH model

Figure 6a shows that the second and third topographic terms will have the equivalent power as the first term in the degrees 49 and 82, respectively. It means that these terms are not convergent and cannot be used to estimate the atmospheric bias on  $V_{zz}$ . Figures 6b and 6c show that the power of third topographic term is equal to that of the second order one at the

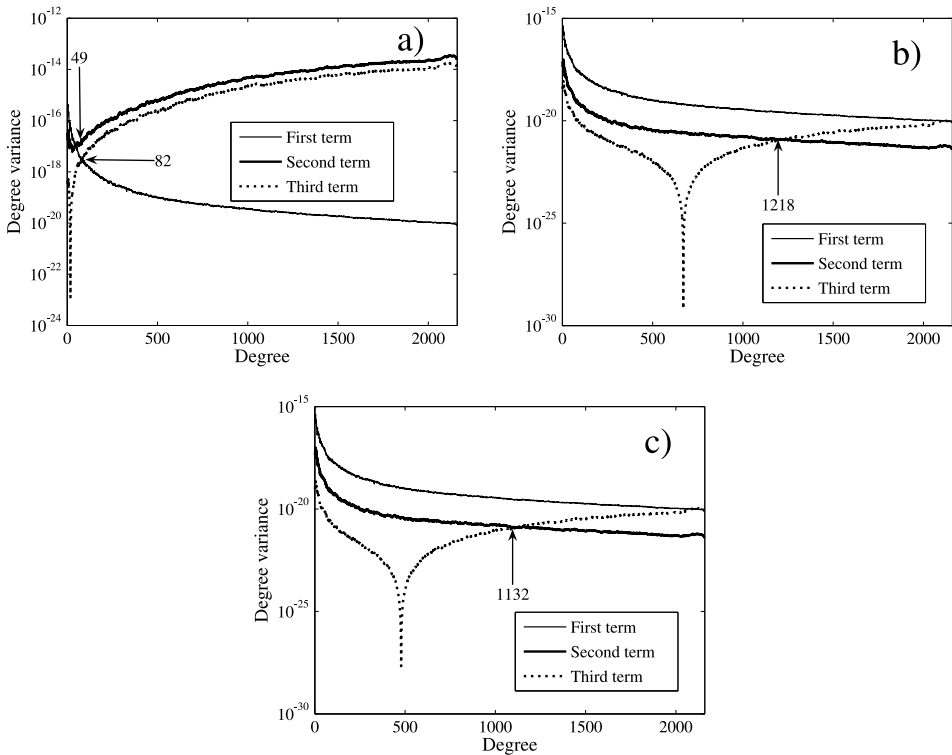


Fig. 6. Degree variances of each topographic term of atmospheric bias based on the KTH model on a)  $V_{zz}$ , b)  $V_{xx}$  and  $V_{yy}$  and c)  $V_{xz}$  and  $V_{yz}$ .

degrees 1218 and 1132 on  $V_{xx}$  and  $V_{yy}$  and  $V_{xz}$  and  $V_{yz}$ , respectively. It will have the same power as the first term for the degree greater than 2000 but will not be important as it is of the same power as the second term.

A general conclusion can be made for the convergence of the atmospheric bias on the gravitational gradients based on all the considered analytical atmospheric density models. The harmonic coefficients of the atmospheric bias on  $V_{zz}$  converge if the first topographic term is used in the mathematical expression of the bias. Correspondingly, the harmonics of the atmospheric bias on  $V_{xx}$ ,  $V_{yy}$ ,  $V_{xz}$  and  $V_{yz}$  will converge when the binomial expansion of the topographic heights is considered to third-order; namely, if the first and second topographic terms of the harmonics are considered. More precisely, we can say that the atmospheric bias on  $V_{zz}$  is convergent to degrees 95, 88 and 49 based on the power, exponential and KTH models, respectively, to the second topographic term, or they are asymptotically convergent to the third term. This degree is 58 for the topographic bias on the same gradients. The topographic and atmospheric biases on  $V_{xx}$  and  $V_{yy}$  are convergent to the second topographic term and asymptotically convergent to the third term for the degrees below 66 for the topographic bias, and below 1447, 888 and 1218 for the atmospheric bias based on the power, exponential and KTH models, respectively. These numbers are 114 for the topographic bias and 1447, 1298 and 1132 for the atmospheric bias on  $V_{xz}$  and  $V_{yz}$ .

From the above study we can conclude that for continuing the gravitational gradients down to sea level based on analytical continuation, the topographic and atmospheric biases should be considered just to first topographic term for  $V_{zz}$ , and to second term for  $V_{xx}$ ,  $V_{yy}$ ,  $V_{xz}$  and  $V_{yz}$  and there is no difficulty in convergence of harmonic for  $V_{xy}$ . The gravitational gradient can be continued analytically (without removing and restoring the topographic and atmospheric effects), but the topographic and atmospheric biases should be removed from the downward continued gradients (which are biased) at sea level.

## 6. Conclusions

We presented the mathematical models of the atmospheric and topographic biases on the gravitational gradients. We showed that the harmonics of the

biases are convergent if the binomial expansion of the topographic heights is truncated to third order. The harmonics of the atmospheric bias of  $V_{zz}$  is convergent just to the first topographic term. It means that for computing the atmospheric bias the harmonics should be generated to this term, independent of the altitude of gradiometer and application. There is no convergence difficulty in  $V_{xy}$  and it can be continued downward to sea level analytically and the biases can be removed from the results; it is not important at which altitude the gravity gradients are measured. The harmonics of the atmospheric bias of the other gradients are convergent to the second order topographic term and they are asymptotically convergent to the third term. It means that the harmonics should be generated to the second term when the gravity gradients are measured near the Earth's surface but for the satellite gravity gradiometry missions, e.g., GOCE, the third term can also be used as the GOCE data cannot sense higher frequencies of the Earth gravity field and the maximum degree of the gravity field is smaller than the convergence degree.

***Acknowledgments.*** The author would like to thank Professor Lars E. Sjöberg for his idea about theory of topographic and atmospheric biases. The Swedish National Space Board is acknowledged for the financial support, project No. 63/07:1. Both unknown reviewers are acknowledged for the constructive comments on the manuscript.

## References

- Albertella A., Migliaccio F., Sansò F., 2002: GOCE: The Earth Field by Space Gradiometry. *Celestial Mechanics and Dynamical Astronomy*, **83**, 1–15.
- Balmino G., Perosanz F., Rummel R., Sneeuw N., Sünkel H., Woodworth P., 1998: European Views on Dedicated Gravity Field Missions: GRACE and GOCE. An Earth Sciences Division Consultation Document, ESA, ESD-MAG-REP-CON-001.
- Balmino G., Perosanz F., Rummel R., Sneeuw N., Sünkel H., 2001: CHAMP, GRACE and GOCE: Mission Concepts and Simulations. *Boll. Geof. Teor. Appl.*, **40**, 3-4, 309–320.
- Ecker E., Mittermayer E., 1969: Gravity corrections for the influence of the atmosphere. *Bollettino di Geofisica Teorica ed Applicata*, **11**, 70–80.
- ESA, 1999: Gravity Field and Steady-State Ocean Circulation Mission, ESA SP-1233(1), Report for mission selection of the four candidate earth explorer missions. ESA Publications Division, p. 217.

- Eshagh M., 2009a: On satellite gravity gradiometry. Doctoral dissertation in Geodesy, Royal Institute of Technology (KTH), Stockholm, Sweden.
- Eshagh M., 2009b: Spherical harmonic expansion of the atmospheric gravitational potential based on exponential and power models of atmosphere. *Artificial Satellites*, **43**, 1, 25–43.
- Eshagh M., Sjöberg L. E., 2008: Impact of topographic and atmospheric masses over Iran on validation and inversion of GOCE gradiometric data. *J. Earth. & Space. Phys.* **34**, 3, 15–30.
- Eshagh M., Sjöberg L. E., 2009a: Topographic and atmospheric effects on GOCE gradiometric data in a local north-oriented frame: A case study in Fennoscandia and Iran. *Studia Geophys. et Geodaet.*, **53**, 61–80.
- Eshagh M., Sjöberg L. E., 2009b: Atmospheric effect on satellite gravity gradiometry data, *Journal of Geodynamics*, **47**, 9–19.
- Heck B., 2003: On Helmert's Methods of Condensation. *Journal of Geodesy*, **7**, 155–170.
- Heiskanen W., Moritz H., 1967: *Physical Geodesy*. W. H Freeman and company, San Francisco and London.
- Lambeck K., 1988: *Geophysical geodesy, the slow deformations of the Earth*. Clarendon, Oxford University Press, New York.
- Makhloof A., 2007: The use of topographic-isostatic mass information in geodetic applications. Doctoral dissertation, Dept. of Theoretical and Physical Geodesy, Bonn, Germany.
- Makhloof A., Ilk K. H., 2005: Far-zone topography effects on gravity and geoid heights according to Helmert's methods of condensation and based on Airy-Heiskanen model. Proceedings the 3<sup>rd</sup> minia International conference for advanced trends in Engineering, El-Minia, April 3-5, 2005.
- Makhloof A., Ilk K. H., 2006: Band-limited topography effects in airborne gravimetry using space localizing base functions. EGU conference, 3 April, 2006.
- Martinec Z., Matyska C., Grafarend E. W., Vaníček P., 1993: On Helmert's 2<sup>nd</sup> condensation method, *Manuscripta Geodaetica*, **18**, 417–421.
- Martinec Z., Vaníček P., 1994: Direct topographical effect of Helmert's condensation for a spherical geoid. *Manuscripta Geodaetica*, **19**, 257–268.
- Moritz H., 1980: *Advanced physical geodesy*. Herbert Wichman, Karlsruhe.
- Novák P., 2000: Evaluation of gravity data for the Stokes-Helmert solution to the geodetic boundary-value problem. Technical Report 207, Department of Geodesy and Geomatics Engineering, University of New Brunswick, Fredericton, Canada.
- Novák P., Grafarend E. W., 2006: The effect of topographical and atmospheric masses on spaceborne gravimetric and gradiometric data. *Studia Geophys. et Geodaet.*, **50**, 549–582.
- Reed G. B., 1973: Application of kinematical geodesy for determining the short wavelength component of the gravity field by satellite gradiometry. Ohio State University, Dept. of Geod Science, Rep. No. 201, Columbus, Ohio.
- Reference Atmosphere Committee, 1961: Report of the preparatory group for an international reference atmosphere accepted at the COSPAR Meeting in Florance, April 1961. North Holland Publ. Co., Amsterdam.

- Rummel R., Rapp R. H., Sünkel H., 1998: Comparisons of global topographic/isostatic models to the Earth's observed gravity field. Ohio State University, Dept. of Geod Science, Rep. No. 388, Columbus, Ohio.
- Seitz K., Heck B., 2003: Efficient calculation of topographic reductions by the use of tesseroids. Presentation at the joint assembly of the EGS, AGU and EUG, Nice, France, 6–11 April 2003.
- Sjöberg L. E., 1984: Least-Squares modification of Stokes' and Vening-Meinez' formula by accounting for truncation and potential coefficients errors. *Manuscripta Geodaetica*, **9**, 209–229.
- Sjöberg L. E., 1991: Refined least-squares modification of Stokes' formula. *Manuscripta Geodaetica*, **16**, 367–375.
- Sjöberg L. E., 2003: A general model for modifying Stokes' formula and its least-squares solution. *Journal of Geodesy*, **77**, 459–464.
- Sjöberg L. E., 1993: Terrain effects in the atmospheric gravity and geoid correction. *Bulletin Geodesique*, **64**, 178–184.
- Sjöberg L. E., 1998: The ellipsoidal corrections to the topographic geoid effects. *Journal of Geodesy*, **77**, 804–808.
- Sjöberg L. E., 1998: The atmospheric geoid and gravity corrections. *Bollettino di geodesia e scienze affini*, **57**, 4, 421–435.
- Sjöberg L. E., 1999: The IAG approach to the atmospheric geoid correction in Stokes's formula and a new strategy. *Journal of Geodesy*, **73**, 362–366.
- Sjöberg L. E., 2000: Topographic effects by the Stokes-Helmert method of geoid and quasi-geoid determinations. *Journal of Geodesy*, **74**, 255–268.
- Sjöberg L. E., 2001: Topographic and atmospheric corrections of gravimetric geoid determination with special emphasis on the effects of harmonics of degrees zero and one. *Journal of Geodesy*, **75**, 283–290.
- Sjöberg L. E., 2006: The effects of Stokes's formula for an ellipsoidal layering of the earth's atmosphere. *Journal of Geodesy*, **79**, 675–681.
- Sjöberg L. E., 2007: Topographic bias by analytical continuation in physical geodesy. *Journal of Geodesy*, **81**, 345–350.
- Sjöberg L. E., 2008: Answers to the comments by M. Vermeer on L. E. Sjöberg (2007) "The topographic bias in physical geodesy". *Journal of Geodesy*, **81**, 345–350.
- Sjöberg L. E., 2009a: Terrain correction in gravimetric geoid computation - is it needed? *Geophys. J. Int.*, **176**, 12–18.
- Sjöberg L. E., 2009b: On the topographic bias in geoid determination by the external gravity field. *Journal of Geodesy* (on line).
- Sjöberg L. E., Nahavandchi H., 1999: On the indirect effect in the Stokes-Helmert method of geoid determination. *Journal of Geodesy*, **73**, 87–93.
- Sjöberg L. E., Nahavandchi H., 2000: The atmospheric geoid effects in Stokes formula. *Geophysical Journal International*, **140**, 95–100.
- Tenzer R., Novák P., Moore P., Vajda P., 2006: Atmospheric effects in the derivation of geoid-generated gravity anomalies. *Studia Geophys. et Geodaet.*, **50**, 583–593.

- 
- Tsoulis D., 2001: Terrain correction computations for a densely sampled DTM in the Bavarian Alps. *Journal of Geodesy*, **75**, 5-6, 291–307.
- United States Standard Atmosphere, 1976: Joint model of the National Oceanic and Atmospheric administration, national aeronautics and space administration and United States air force, Washington, D. C.
- Vermeer M., 2008: Comment on L. E. Sjöberg (2006): The topographic bias by analytical continuation in physical geodesy. *Journal of Geodesy*, **81**, 5, 345–350.
- Wallace J. M., Hobbs P. V., 1977: *Atmospheric Science - An Introductory Survey*, Academic press, New York.
- Wieczorek M. A., 2007: The gravity and topography of the terrestrial planets. *Treatise on Geophysics*, **10**, 165–206.
- Wild F., Heck B., 2004a: A comparison of different isostatic models applied to satellite gravity gradiometry, Gravity, Geoid and Space Missions GGSM 2004 IAG International Symposium Porto, Portugal August 30-September 3, 2004.
- Wild F., Heck B., 2004b: Effects of topographic and isostatic masses in satellite gravity gradiometry. Proc. Second International GOCE User Workshop GOCE. The Geoid and Oceanography, ESA-ESRIN, Frascati/Italy, March 8-10, 2004 (ESA SP – 569, June 2004), CD-ROM.